Science objectives and first results from the SMART-1/AMIE multicolour micro-camera

J.-L. Josset [a], S. Beauvivre [a,*], P. Cerroni [b], M.C. De Sanctis [b], P. Pinet [c], S. Chevrel [c], Y. Langevin [d], M.A. Barucci [e], P. Plancke [f], D. Koschny [f], M. Almeida [f], Z. Sodnik [f], S. Mancuso [f], B.A. Hofmann [g], K. Muinonen [h], V. Shevchenko [i], Yu. Shkuratov [j], P. Ehrenfreund [k], B.H. Foing [f]

[a] *SPACE-X, Space Exploration Institute, Jaquet Droz 1, Neuchâtel, Switzerland*
[b] *IASF – Area Ricerca Cnr, Via Fosso del Cavaliere, 00133 Roma, Italy*
[c] *UMR 5562 "Dynamique Terrestre et Planétaire", CNRS/Université Paul Sabatier, GRGS (Groupe de Recherche en Géodésie Spatiale), Observatoire Midi-Pyrénées, 14, avenue Edouard Belin, 31400 Toulouse, France*
[d] *IAS – Bat. 121, 91405 Orsay, France*
[e] *Observatoire Paris Meudon (OBSPM), Meudon, France*
[f] *ESA/ESTEC, Keplerlaan 1, 2201 Noordwijk, The Netherlands*
[g] *Natural History Museum, Bern, Switzerland*
[h] *Helsinki Observatory, Kopernikuk sentie 1, P.O. Box 14, Finland*
[i] *Sternberg Astronomical Institute, Moscow 119899, Russia*
[j] *Astronomical Institute of Kharkov National University, 35 Sumskaya St., Kharkov 61022, Ukraine*
[k] *Leiden Observatory and Austrian Academy of Sciences, P.O. Box 9513, 2300 RA Leiden, The Netherlands*

Abstract

The Advanced Moon micro-Imager Experiment (AMIE), on-board SMART-1, the first European mission to the Moon, is an imaging system with scientific, technical and public outreach objectives. The science objectives are to image the lunar South Pole, permanent shadow areas (ice deposit), eternal light (crater rims), ancient lunar non-mare volcanism, local spectrophotometry and physical state of the lunar surface, and to map high latitudes regions (south) mainly at far side (South Pole Aitken basin). The technical objectives are to perform a Laserlink experiment (detection of laser beam emitted by ESA/Tenerife ground station), flight demonstration of new technologies and on-board autonomy navigation. The public outreach and educational objectives are to promote planetary exploration and space. We present here the first results obtained during the cruise phase.
© 2005 Published by Elsevier Ltd on behalf of COSPAR.

Keywords: Moon; SMART-1; Camera; Exploration

1. Introduction

The Advanced Moon micro-Imager Experiment (AMIE) is the imaging system on-board ESA mission to the Moon SMART-1; it makes use of a miniaturised micro-camera and micro-processor electronics developed by SPACE-X, Space Exploration Institute, CH-Neuchâtel, based on developments made in the frame of the ESA technological research programme. The AMIE camera will provide high resolution CCD images of selected lunar areas and it will perform colour imaging through three filters at 750, 915 and 960 nm with a

* Corresponding author. Tel.: +41 32 720 5604; fax: +41 32 720 5737.
E-mail address: stephane.beauvivre@space-x.ch (S. Beauvivre).

maximum resolution of 27 m/pixel at the perilune of 300 km. Specific scientific objectives include (1) imaging of the lunar South Pole, study of permanently shadowed regions (2) imaging features of the far side and in particular the South Pole Aitken basin (SPA) (3) study of photometric properties of the lunar surface from observations at different phase angles for the determination of the regolithic structure parameters, (4) prognosis of chemical and mineral composition of the regolith upper layer, (5) detection and characterisation of lunar non-mare volcanic units, (6) study of lithological variations from impact craters and implications for crustal heterogeneity. The AMIE camera also supports a Laserlink experiment to Earth, an On-Board Autonomous Navigation investigation and a lunar libration experiment coordinated with radio science measurements. Finally, AMIE will provide the spatial and geologic context for the compositional data acquired by the spectrometer SIR on-board SMART-1.

2. The AMIE camera

The AMIE imaging system is constituted of two units, a camera unit and a dedicated electronics unit (Fig. 1). The camera includes a tele-objective with a $5.3° \times 5.3°$ field of view and an imaging sensor of 1024×1024 pixels. The AMIE camera will acquire images in three spectral filters, at wavelengths of 750, 915 and 960 nm; the filters are directly in front of the CCD covering an area of 11/16 of the total CCD area, with one 1/16 used by the laser filter at 847 nm, while the remaining 512×512 pixels (i.e., 1/4 of the CCD area) are not covered by filters and thus devoted to total light imaging. It should be noted that while the filters at 750 and 915 nm are two narrow-band filters (respective width 10 and 30 nm), that at 960 nm is a high-pass filter with steep transmission edge which critically convolves with the negative slope of the CCD spectral response in the longer wavelengths region of the spectrum. The layout of the filters on the CCD is shown in Fig. 2;
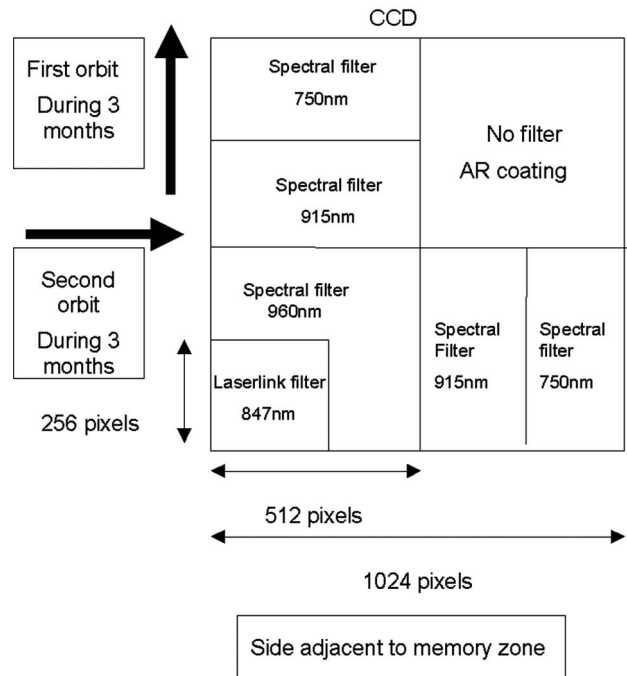
Fig. 2. Filters.

the filters disposition allows a mapping of the lunar surface during the 2 orbit configurations around the Moon, i.e. it allows the same region on the lunar surface to be imaged in the three spectral filters during the two different orbital attitudes.

The dedicated electronic unit insures the following functions: (i) data control and power management of the camera; (ii) image data storage into a mass memory buffer; (iii) data control and power management of a cube Micro-DPU (image processing, e.g. compression); (iv) communication with the S/C through the S/C CAN Bus Interface; (v) adaptation of the S/C supply voltage (S/C Power Bus Interface) to the levels required by its electronics and the camera.

AMIE performances are:

- $5.3° \times 5.3°$ FOV → Images 45 km × 45 km at 500 km
- CCD 1024×1024 → resolution 45 m/pixel at 500 km with 10 bits/pixel
- Powerful image compression unit → high data compression rate
- Power supply I/F board (PSIF)
- System control unit (SCU): μP board, buffer memory…
- Specific radiation shielding
- Total mass 2 kg

The nominal operational lunar orbit of the spacecraft SMART-1 will be polar, with the perilune lowest altitude at approximately 300 km and apolune at 3000 km. At a distance of 300 km, the field of view of

Fig. 1. AMIE Imaging System.

AMIE ($5.3° \times 5.3°$) corresponds to 27 km: the spatial resolution for the 1024×1024 CCD is therefore 27 m at perilune.

3. Scientific objectives

The AMIE camera will carry out both scientific objectives and technological objectives. The AMIE camera will produce multicolour images in three spectral bands, thus allowing us to discriminate by the Fe^{2+} absorption feature at 0.95 μm between mafic minerals (pyroxenes, olivines) that compose the mare and highland materials. It will also be possible to study surface alteration processes on the lunar surface, under the influence of the solar wind and micro-meteorites (the maturation processes). The possibility for reliable prognosis of chemical/mineral composition and maturity degree of the lunar surface materials using AMIE/SMART-1 filters was shown in (Shkuratov et al., 2003a).

The investigation by the AMIE micro-camera will address a number of specific scientific objectives.

3.1. Detailed high resolution imaging of the South Pole

The South Polar Region is one of the priority targets of the mission. The possibility of ice deposits in the permanently shadowed regions in the South Pole was put forward as a probable explanation for results from the Clementine Bistatic radar experiment (Nozette et al., 1996) and seems to be confirmed by the results of the lunar prospector neutron spectrometer (Feldman et al., 2001). Icy deposits can exist in "double shadow" regions, i.e. small craters in permanently shadowed areas, which protect the deposit from sunlight diffused by the rims, though these deposits can survive not only in double shadowed regions (Vasavada et al., 1999). Furthermore, the South at farside is on the rim of a major geologic feature, the South Pole Aitken basin, more than 2500 km in diameter, the largest such feature on the Moon (see the discussion in Head et al., 1993 and Pieters et al., 1993). The impact event which produced South Pole Aitken basin penetrated very deep into the far side crust, but the basin was not filled up by lava flows as was the case for similar features on the near side. There is therefore a strong interest in investigating at close range the mineralogical composition of ejecta, which provide a vertical view of the far side crust down to several 10 km. Images in the three AMIE filters could be used to search for cryptomaria (Head and Wilson, 1992; Yingst and Head, 1997) around dark halo craters in the SPA region. AMIE will directly contribute to the characterisation of surface mineralogy and geology in the SPA region, in combination with other elements of the SMART-1 payload.

3.2. Study of lithological compositional diversity across the exposed walls of impact craters

Compositional heterogeneities have been observed in morphological structures (central peaks, floor, walls, rims) of impact craters: indeed, a global survey of central peaks of 109 craters (Tompkins and Pieters, 1999) in the diameter range from 40 to 180 km has shown that 40% of them exhibit multiple lithology, considered to be associated with vertical and lateral differences in the composition of the lunar crust. The characterisation of structural lithological variations on the walls of large impact craters, such as Copernicus shown by multispectral telescopic then Clementine images (Pinet et al., 1993; Pieters et al., 1994) or complex lithological variations observed for example in Aristarchus (see, e.g., Pinet et al., 1999; Le Mouelic et al., 2000; Chevrel et al., 2004) could be significantly improved at a spatial resolution of 50 m/pixel scale. New higher resolution data from AMIE, combined with spectroscopic information from SIR, could identify combination of smaller, lithologically distinct units within their central peaks and walls. The characterization and the distribution of fresh crater materials (including the ejecta blanket), respectively at high spatial and spectral resolution by AMIE and SIR, will also contribute to better document the processes of excavation and production of impact materials (e.g., abundance of rocks versus melt products).

3.3. Detection and characterisation of the ancient lunar non-mare volcanism

While lunar mare volcanism appears both widespread and well documented, little is known about the emplacement of lunar non-mare volcanic units before and during the period of mare basaltic volcanism (Head and Wilson, 1992). The best candidates today for non-mare volcanic deposits are a number of small lunar areas called red spots characterised by a relatively high albedo and a strong absorption in the UV relative to the visible (Malin, 1974; Chevrel et al., 1999; Hawke et al., 2003; Wilson and Head, 2003). The AMIE camera will provide high spatial resolution imaging associated with different geometry conditions of observation and combined with multispectral mapping, giving access to mineralogy, morphology and surface physical characteristics.

3.4. Physical properties of regolith

The lunar regolith is a complex end-product of the bombardment history of the Moon: lunar surface materials were fractured, melted, welded (forming complex breccias) and displaced during the major cratering events, and reworked during the smaller ones. For this

reason, it is difficult to understand the regolith evolution, its distribution on the Moon or its depth. A detailed study of the lunar regolith provides a key for understanding the soil maturation processes including impact comminution, accumulation of agglutinates, and production of reduced iron from vacuum reduction of Fe^{2+} in minerals and glasses. The study of the regolith distribution requires high resolution imaging. Observations planned at different phase angles during the SMART-1 mission, will allow us to study the photometric properties of the regolith, from which physical properties of the surface can be inferred (see, e.g., Pinet et al., 2000; Shkuratov et al., 1999, 2003b; Muinonen et al., 2002; Kreslavsky and Shkuratov, 2003).

Three different kind of photometric studies with the AMIE camera of SMART-1 mission will be possible: (1) mapping slope of phase function, (2) studying the opposition spike, and (3) detailed study of photometric function in tracking mode of SMART-1. The first kind allows studies of photometric anomalies related to fresh impact craters for estimates of the regolith gardening rate and projectile flux in recent epoch; investigations of regolith structure anomalies associated with swirl, searching for evidences of recent seismic events. The second kind makes possible the study of regional variations of the characteristic soil particle size and particle aggregate structure. The third one (tracking mode or spot pointing) allows us to perform detailed study of photometric function giving information about meso-scale structure of the lunar surface. These observations will improve our understanding of the subsurface regolith layering and reworking.

A more detailed description of scientific objectives and expected results for the AMIE camera in lunar orbit is given in Pinet et al. (2005).

4. First results

Numerous images have been taken since the launch in September 2003, as part of the pre-commissioning and commissioning, Laserlink experiment, OBAN experiment, Earth and Moon imaging.

Pre-commissioning was performed on 3 October 2003. It was intended to verify the health of the instrument after launch. The entire process of the pre-commissioning was performed nominally and as planned. After AMIE System Control Unit (SCU) had been switched on by the spacecraft, several commands were sent to AMIE allowing switching on and off the AMIE subsystems: the Camera and the Image Compression Unit (ICU). In particular, a specific "diagnostic" command allowed checking deeply the electrical behavior of the complete imaging system. All the results were nominal. The data downloaded from AMIE have shown the good electrical behavior of the instrument, as well as some

indication on the good physical condition of the filters and the data acquisition chain. The power consumption was nominal with respect to the various AMIE configurations.

In-flight calibration has been performed during commissioning (bright star imaging in all filters, Moon imaging in all filters, uncompressed Moon images, flat fields, AMIE-SIR coalignment). Preliminary results show that the camera performance is more or less unchanged with respect to the ground performance. The number of bad pixels increased, as expected – but still the number of bad pixels is very small, which will not affect the science return. Fig. 3 shows one of the results – the image of the standard star Vega in the none filter area of the detector. So far only in one image, we measured the Point Spread Function of the star to be 1.20 pixels, which is in excellent agreement with the ground-based value of (1.21 ± 0.06) pixels. The lunar images show that we can indeed image extended objects. Fig. 4 shows an example of two ratio images of different wavelengths (colour indexes $0.915/0.75\ \mu m$ and $0.96/0.75\ \mu m$). As has been shown (Shkuratov et al., 2003a), these colour indexes can be potentially used to map the Fe content and maturity degree of the lunar soil (see Fig. 2 for a definition of the filter names). Again, these were uncalibrated images. We checked the deviations of the ratio to the mean value, and the numbers are well within the expected values, giving us high confidence that we will be able to perform the mineralogical studies planned with the camera.

During the Earth Escape phase, many images of the Moon and the Earth have been taken. In the first picture of the Moon, shown in Fig. 5, taken on 18 January 2004, it is possible to identify Grimaldi crater and Mare Humorum. Numerous views of the Earth have been
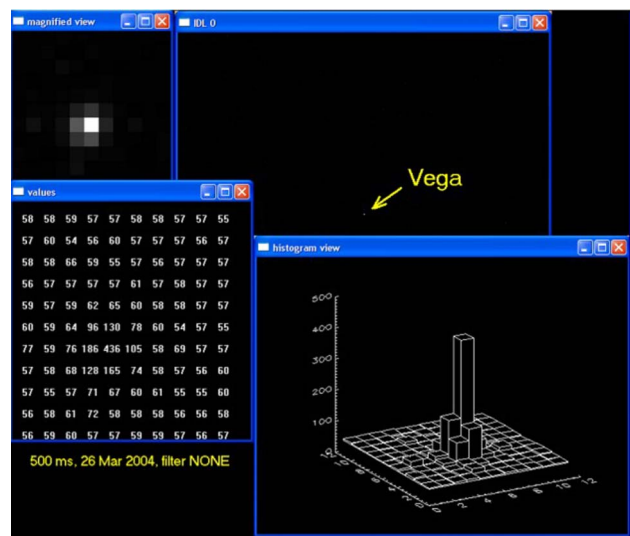
Fig. 3. The star Vega in the none filter area of AMIE. 500 ms exposure.
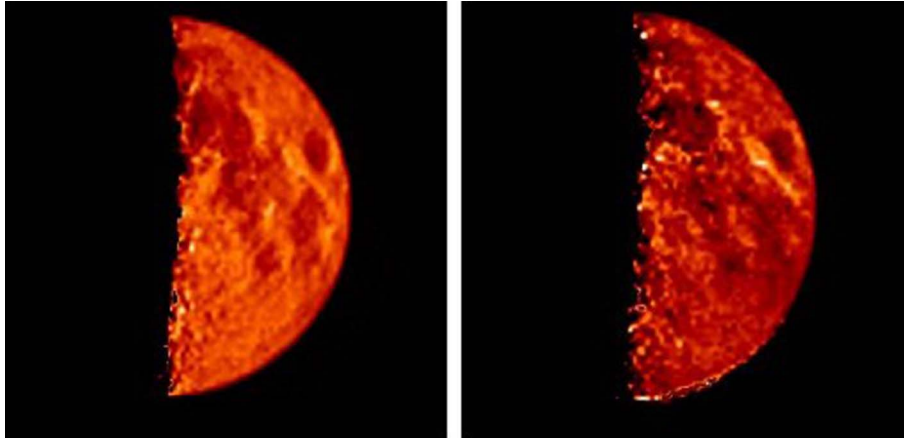
Fig. 4. Ratios images FeH/VIS (left) and FeL/VIS (right).

obtained, with different scales, depending on the position of the spacecraft on its elliptical orbit. Fig. 6 shows an image taken at about 110,000 km from the Earth. This large view from Europe to Sri Lanka, taken in a single shot, covers half of the image taken by AMIE and covers 4 filters.
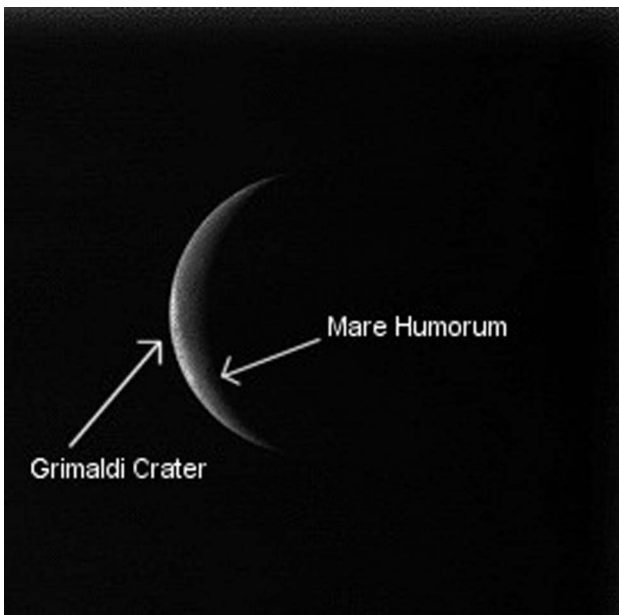
Fig. 5. First Moon picture taken with the AMIE Camera.
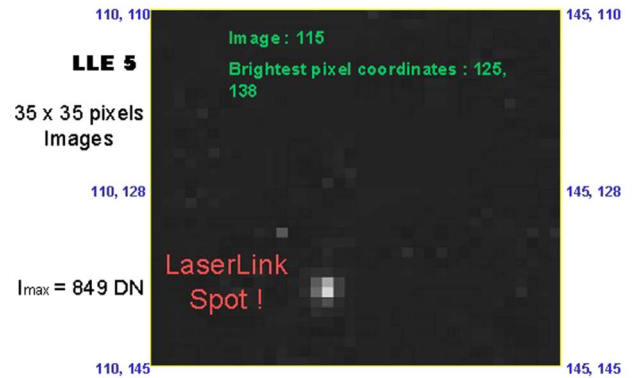
Fig. 7. Laserlink spot acquired at 50,000 km from the Earth.

Fig. 6. Earth taken by AMIE on 21 June 2004 at 110,000 km from Earth.

In February 2004, a Laserlink experiment was performed at ~50,000 km from the Earth. Fig. 7 shows the laser spot in the specific dedicated area of the detector.

5. Conclusions

The AMIE experiment on-board the SMART-1 mission is a new generation of advanced imaging system, combining a miniaturised detector with micro-processor electronics. First results from pre-commissioning, commissioning and cruise science indicate that AMIE is performing nominally and that it will be able to achieve its scientific objectives during the lunar observation phase starting with the commissioning of the instruments in lunar orbit from January 15th 2005.

Specific scientific objectives for lunar imaging will include (i) the detailed imaging of the lunar South Pole and study of permanently shadowed regions, (ii) imaging features of the far side and in particular the South Pole Aitken basin (SPA) (iii) the study of photometric properties of the lunar surface from observations at different phase angles for the determination of the regolithic structure parameters, (iv) the prognosis of chemical and mineral composition of the regolith upper layer, (v) the detection and characterisation of lunar non-mare volcanic units, (vi) the study of the local lithological variations from impact craters and implications for crustal heterogeneity.

Laserlink and OBAN experiments were successfully performed during cruise.

References

Chevrel, S.D., Pinet, P.C., Head, J.W. Gruithuisen domes region: a candidate for an extended non-mare volcanism unit on the Moon. Journal of Geophysical Research 104, 16515–16529, 1999.

Chevrel, S.D., Pinet, P.C., Daydou, Y., Baratoux, D., Costard, F., Le Moué lic, S., Langevin, Y., Erard, S., Compositional and structural study of the Aristarchus Plateau from integrated UV–Vis–NIR spectral data, in: Proceedings of the LPSC 35th, 2004.

Feldman, W.C., Maurice, S., Lawrence, D.J., Little, R.C., Lawson, S.L., Gasnault, O., Wiens, R.C., Barraclough, B.L., Elphic, R.C., Prettyman, T.H., Steinberg, J.T., Binder, A.B. Evidence for water ice near the lunar poles. Journal of Geophysical Research – Planets 106 (E10), 23232–23252, 2001.

Hawke, B.R., Lawrence, D.J., Blewett, D.T., Lucey, P.G., Smith, G.A., Spudis, P.D., Taylor, G.J. Hansteen Alpha: A volcanic construct in the lunar highlands. Journal of Geophysical Research 108 (E7), 5069, doi:10.1029/2002JE002013, 2003.

Head, J.W., Wilson, L. Lunar mare volcanism: Stratigraphy, eruption conditions, and the evolution of secondary crusts. Geochimica et Cosmochimica Acta 55, 2155–2175, 1992.

Head, J.W., Murchie, S., Mustard, J.F., Pieters, C.M., Neukum, G., McEwen, A., Greeley, R., Nagel, E., Belton, M.J.S. Lunar impact basins: New data for the western limb and far side (Orientale and South Pole-Aitken basins) from the first Galileo flyby. Journal of Geophysical Research 98, 17,149–17,181, 1993.

Kreslavsky, M., Shkuratov, Yu. Photometric anomalies of the lunar surface: results from Clementine data. Journal of Geophysical Research 108 (E3), 1-1–1-13, 2003.

Le Mouelic, S., Langevin, Y., Erard, S., Pinet, P.C., Daydou, Y., Chevrel, S. Discrimination between maturity and composition of lunar soils from integrated Clementine UV–Vis–NIR data. Application to Aristarchus Plateau. Journal of Geophysical Research 105 (E4), 9445–9455, 2000.

Malin, M.C. Lunar red spots: Possible pre-mare materials. Earth Planetary Science Letters 21, 331–341, 1974.

Muinonen, K., Shkuratov, Yu., Ovcharenko, A., Piironen, J., Stankevich, D., Miloslavskaya, O., Keraenen, S., Josset, J.-L. The SMART-1 AMIE experiment: implication to the lunar opposition effect. Planetary Space Science, 1339–1344, 2002.

Nozette, S., Lichtenberg, C.L., Spudis, P., Bonner, R., Ort, W., Malaret, E., Robinson, M., Shoemaker, E.M. The Clementine Bistatic Radar Experiment. Science 274 (5292), 1495–1498, 1996.

Pieters, C.M, Head, J.W., Sunshine, J.M., Fischer, E.M., Murchie, S.L., Belton, M., McEwen, A., Gaddis, L., Greeley, R., Neukum, G., Jaumann, R., Hoffmann, H. Crustal diversity of the Moon: Compositional analyses of Galileo Solid State Imaging data. Journal of Geophysical Research 98, 17127–17148, 1993.

Pieters, C.M., Staid, M.I., Fisher, E.M., Tompkins, S., He, G. A sharper view of impact craters from Clementine data. Science 266, 1844–1848, 1994.

Pinet, P.C., Chevrel, S., Martin, P. Copernicus – a regional probe of the lunar interior. Science 260, 797–801, 1993.

Pinet, P.C., Shevchenko, V.V., Chevrel, S.D., Daydou, Y., Rosemberg, C. Local and regional lunar regolith characteristics at Reiner Gamma Formation: optical and spectroscopic properties from Clementine and Earth-based data. Journal of Geophysical Research 105, 9457–9475, 2000.

Pinet, P.C., Cerroni, P., Josset, J.-L., Beauvivre, S., Chevrel, S., Muinonen, K., Piironen, J., Langevin, Y., Barucci, M.A., De Sanctis, M.C., Shkuratov, Yu., Shevchenko, V., Plancke, P., Hofmann, B.A., Josset, M., Ehrenfreund, P., Sodnik, Z., Koschny, D., Almeida, M., Foing, B. The advanced moon micro-imager experiment (AMIE) on SMART-1: scientific goals and expected results. Planet and Space Science, accepted for publication, 2005, in press.

Pinet, P.C., Chevrel, S.C., Daydou, Y.H., Lemouelic, S., Langevin, Y., Erard, S., Aristarchus crater: spectroscopic heterogeneity from Clementine UV–VIS–NIR data, in: Lunar and Planet. Science Conference, 30th, Houston, TX, Contribution, #1555, 1999.

Shkuratov, Yu., Kreslavsky, M., Ovcharenko, A., Stankevich, D., Zubko, E., Pieters, C., Arnold, G. Opposition effect from Clementine data and mechanisms of backscatter. Icarus 141, 132–155, 1999.

Shkuratov, Yu., Stankevich, D., Kaydash, V., Omelchenko, V., Pieters, C., Pinet, P., Chevrel, S., Daydou, Y., Foing, B., Sodnik, Z., Josset, J.-L., Taylor, L., Shevchenko, V. Composition the lunar surface as will be seen from SMART-1: simulation using Clemen-

tine data. Journal of Geophysical Research – Planets 108 (E4), 1-1–1-12.

Shkuratov, Yu.G., Kreslavsky, M.A., Stankevich, D.G., Kaydash, V.G., Pinet, P., Shevchenko, V.V., Foing, B.H., Josset, J.-L. The SMART-1 mission: photometric studies of the Moon with the AMIE camera. Solar System Research 37, 251–259, 2003b.

Tompkins, S., Pieters, C. Mineralogy of the lunar crust: results from Clementine. Meteoritics and Planetary Sciences 34, 25–41, 1999.

Vasavada, A.R., Paige, D.A., Wood, S.E. Near-surface temperatures on Mercury and the Moon and the stability of polar ice deposits. Icarus 141 (October), 179–193, 1999.

Wilson, L., Head, J.W. Lunar Gruithuisen and Mairan domes: Rheology and mode of emplacement. Journal of Geophysical Research 108 (E2), 5012, doi:10.1029/2002JE001909, 2003.

Yingst, R.A., Head, J.W. Volumes of lunar lava ponds in South Pole-Aitken and Orientale Basins: Implications for eruption conditions, transport mechanisms and magma source regions. Journal of Geophysical Research – Planets 102, 10909–10931, 1997.